



A novel chitosan microsphere as food processing enzyme immobilization carrier and its application in nucleotide production

Xiao-Yan Yin^{a,1}, Rui-Fan Yang^{b,1}, Zhong-Hua Yang^{a,*}

^a Xingzhi College, Zhejiang Normal University, Jinhua 321100, China

^b School of Basic Medical Sciences, Capital Medical University, Beijing 100069, China

ARTICLE INFO

Keywords:

Nucleic acid hydrolysis
Nuclease P1
Nucleotide
Enzyme immobilization
Food processing enzyme

ABSTRACT

Developing a robust and safe carrier for enzyme immobilization is crucial for their application in the food processing industry. In this study, a novel crosslinked chitosan microspheres (CSMs) were prepared using glutaraldehyde (GA) as the crosslinking agent, using a newly developed emulsification-neutralization combined method. Nuclease P1 (NP1) was immobilized onto these microspheres, the maximum activity of NP1@CSMs-GA reach to 53,859.4 U/g. The activity recovery yield reach to 75 %. Compared to the free NP1, the stability of NP1@CSMs-GA was significantly enhanced. Its v_{max} and K_m is 895.71 mg/(g·min) and 77.27 mg/mL respectively. This NP1@CSMs-GA was utilized in production of nucleotides through hydrolysis of RNA. In BSTR, NP1@CSMs-GA retained more than 75.1 % initial activity after 10 cycles of reuse. Moreover, in PBR, the RNA hydrolysis conversion rate maintained 81 % after 24 h of continuous operation. These results demonstrate that NP1@CSMs-GA exhibits excellent reusability and production stability in practical processes.

1. Introduction

In the food processing industry, various enzymes are utilized during production processes due to their advantages, including high efficiency, health benefits, and safety. Presently, numerous enzymes have found successful applications in the food sector. For instance, amylase and glucose isomerase are used in the production of syrups, lactase and chymosin are used for produce dairy products, pectinase are used for winemaking, and nuclease and adenylate deaminase are used in condiments (Collados et al., 2020; Raveendran et al., 2018). Currently, these enzymes are usually used in their free form in food industry. The main demerits of free enzyme are high cost, difficult separation and low stability, which are particularly prominent in the process of large-scale industrial production. The enzyme immobilization technology is an effective route to address these demerits (Atirog, Atiroglu, Atiroglu, Al-Hajri, & Özacar, 2024).

Enzyme immobilization technology offers an effective solution to these issues. Ideally, immobilized enzymes should be reusable, exhibit high enzymatic activity, and maintain stability (W. Zhang et al., 2024). In the context of the food industry, the criteria for immobilized enzymes are even more rigorous. They must be non-toxic, harmless, and possess

good biocompatibility. Additionally, the production process should not generate by-products, and the solid-liquid separation should be straightforward (Atirog et al., 2024; Chalella Mazzocato & Jacquier, 2024; Yushkova et al., 2019). The development of food grade new carrier materials and corresponding immobilization techniques remains a critical area of research for food processing enzyme immobilization (Cavalcante, Cavalcante, de Sousa, Neto, & dos Santos, 2021; Rodrigues, Berenguer-Murcia, Carballares, Morellon-Sterling, & Fernandez-Lafuente, 2021).

Chitosan, a naturally occurring polysaccharide, stands out as an ideal material for enzyme immobilization in the food industry due to its advantages include excellent immobilization properties, non-toxicity, and appropriate price (Dutta, Ravikumar, & Dutta, 2002). The porous network structure of chitosan provides a large specific surface area, and it can be easily processed into various forms, such as films, porous microspheres, nanoparticles, and gels (Krajewska, 2004; Ribeiro, de Farias, Sant'Anna Cadaval Junior, de Almeida Pinto, & Diaz, 2021; Zhou et al., 2023). The abundance of amino and hydroxyl groups in chitosan allows for the formation of covalent bonds with enzyme proteins, facilitating immobilization (Chen & Duan, 2015; Kim & Lee, 2019). When using chitosan as an immobilization matrix, the shape and structure of the

* Corresponding author.

E-mail address: yangzh@zjnu.edu.cn (Z.-H. Yang).

¹ Yin and Yang contributed equally to this work and should be considered as co-first authors.

matrix, which depend on the preparation method, play a vital role in determining its mechanical properties and enzyme loading capacity (Ahmad, Garcia-Rogers, & Moreno, 2022; Aydemir & Guler, 2015; da S. Moreira et al., 2022; Garncarek, 2019; Nunes et al., 2021). Furthermore, the interaction between the enzyme and the chitosan matrix is another important factor to be considered in the immobilization process. (Saravanakumar, Palvannan, Kim, & Park, 2014; Srivastava & Anand, 2014).

5'-Nucleotides are widely used as flavor enhancers in the food industry and pharmaceutical ingredients for antiviral and anticancer drugs in pharmaceutical industry (Liu, Xu, Liang, & Liu, 2020; Wu et al., 2022; J. Zhang et al., 2020). Hydrolysis of RNA into 5'-nucleotides catalyzed by enzyme is the main production route in industry (Benaiges, López-Santin, & Solà, 1990). Nuclease P1 (EC 3.1.30.1, NP1), is a critical enzyme for nucleotide production. In the current industrial practice, NP1 is used in its free form for batch operations (Shi et al., 2009). It is essential to add fresh enzyme for each batch reaction, which remains in the reaction mixture without being separated. This operation leads to high enzyme costs, low productivity, and insufficient product purity which limits its use in pharmaceuticals and other fine chemicals. Additionally, this operation suffers from low efficiency due to start up and shut down procedures, high labor costs or batch to batch variations. Immobilization NP1 can mitigate these shortcomings, making it more suitable for both the food and pharmaceutical sectors (Shi et al., 2010; Shi et al., 2010). The immobilization of NP1 requires a non-toxic, safe, and stable matrix with a high loading capacity, similar to the requirements for conventional enzymes used in food processing. Moreover, the mass transfer resistance of the immobilization matrix will also be considered due to the nature of the substrate, RNA.

In this work, a novel chitosan microsphere was developed for enzyme immobilization through an innovative emulsification-neutralization combined method in food industry. An efficient immobilization technique was developed for the covalent immobilization of NP1 onto this chitosan microsphere. The catalytic performance of the immobilized NP1 was assessed under conditions simulating industrial processes, including recycle in batch stirred tank reactor (BSTR) and continuous packed-bed reactors (PBR), for the hydrolysis of RNA into 5'-nucleotides.

2. Materials and methods

2.1. Materials

Nuclease P1 (NP1) was produced by fermentation with *Penicillium citrinum*. It was preliminarily purified via ammonium sulfate precipitation and followed by ultrafiltration membrane filtration. Yeast RNA was purchased from Shanghai Yuanye Biotechnology Co., Ltd. (Shanghai, China). Chitosan was purchased from Shanghai Ruji Biotechnology Development Co., Ltd. (Shanghai, China). BSA and glutaraldehyde was purchased from Sigma-Aldrich® (Shanghai, China). Sodium acetate, acetic acid, sodium hydroxide, ammonium molybdate, perchloric acid, liquid paraffin, Span-80 and ethanol were purchased from Sinopharm Chemical Reagent Co., Ltd. (Beijing, China).

2.2. Preparation of chitosan microspheres

The chitosan microspheres were prepared using a novel combined method that integrated the emulsification method (Garncarek, 2019) and neutralization method (Ahmad et al., 2022; Aydemir & Guler, 2015). Chitosan 1.5 g was added into 25 mL acetic acid solution (2 %). The mixture was stirred until completely uniform and then allowed to stand at 4 °C for an hour to eliminate bubbles. Subsequently, the chitosan solution was slowly added into a mixture of 50 mL of liquid paraffin containing 0.2 mL of Span-80, and violently stirred to achieve the desired microsphere size. This emulsified solution was then poured into 50 mL of 2 mol/L NaOH solution and further gently stirred to

solidify the microspheres. The chitosan microspheres were collected and washed with deionized water until they reached a neutral pH. Next, the microspheres were cross-linked with a 2.5 % glutaraldehyde solution at 30 °C for 10 min. Afterward, the glutaraldehyde-cross-linked chitosan microspheres (CSMs-GA) were rinsed with deionized water to remove any residual glutaraldehyde. The microspheres were then surface-dried using filter paper and stored at 4 °C for future use.

2.3. Immobilization of nuclease P1 on chitosan microspheres

CSMs-GA, 0.1 g, was added to 4.9 mL of acetic acid buffer (10 mmol/L, pH 5.5). Subsequently, 0.1 mL of NP1 solution (20,000 U/mL) was added into the mixture to facilitate the immobilization of NP1 onto the chitosan microspheres. The immobilization process was carried out for 1 h at 30 °C. Following immobilization, the resulting immobilized enzyme, NP1@CSMs-GA, was washed with an acetic acid buffer solution (10 mmol/L, pH 5.5) at 4 °C. The surface moisture of the NP1@CSMs-GA was carefully removed using filter paper, and the sample was stored at 4 °C.

2.4. Characterization of structure

The morphologies and structures of CSMs-GA and NP1@CSMs-GA were analyzed using a Scanning Electron Microscope (SEM, Apreo S HiVac, Thermo Fisher, Massachusetts, USA) at magnifications of 500×, 10,000×, and 30,000×, with an accelerating voltage of 20 kV. The functional groups of CSMs, CSMs-GA, and NP1@CSMs-GA were further analyzed using Fourier Transform Infrared (FT-IR, INVENIO-R, Bruker, Karlsruhe, Germany) spectroscopy.

2.5. Enzymatic properties of NP1@CSMs-GA

To evaluate the performance of NP1 immobilized on CSMs-GA, a series of enzymatic properties were investigated, including the effects of substrate concentration, as well as the thermal, pH, and storage stability of both free NP1 and NP1@CSMs-GA. Additionally, the kinetic parameters were estimated using the Michaelis-Menten equation (Hoang Hiep & Kim, 2017).

2.6. Application of NP1@CSMs-GA in nucleotide production

The production capacity of NP1@CSMs-GA is evaluated by catalyzing RNA hydrolysis to produce 5'-nucleotides (Benaiges et al., 1990; Shi et al., 2009). Recycles batch operation in a batch stirred tank reactor (BSTR) and continuous operation in a packed-bed reactor (PBR) were applied to simulate industrial production processes.

For the recycles batch operation, 0.5 g of NP1@CSMs-GA with an enzyme activity of 20,000 U/g, and 1000 mL of an 80 g/L RNA solution at pH 5.5 were added into the BSTR. The hydrolysis reaction was carried out for 6 h at 65 °C with a stirring speed of 100 rpm. At the end of each batch, the reaction mixture was filtered. The recovered NP1@CSMs-GA was rinsed with deionized water, and its surface moisture was gently removed using filter paper before being reused in the next cycle. The filtrate was collected, and the residual RNA concentration was determined by spectrophotometry.

In the continuous operation, 0.5 g of NP1@CSMs-GA with an enzyme activity of 20,000 U/g was packed into a PBR equipped with a hot water jacket to maintain a constant reaction temperature of 65 °C. An RNA solution with a pH of 5.5 and a concentration of 50 g/L was continuously fed into the PBR from the bottom at a flow rate of 0.5 mL/min, ensuring a 10-min residence time. Effluent samples were periodically taken, and the RNA hydrolysis rate was determined at set intervals.

2.7. Analysis method

2.7.1. Determination of protein content

The enzyme protein content in the solution was determined using the Coomassie Brilliant Blue method (Buroker-Kilgore & Wang, 1993). Bovine Serum Albumin (BSA) was used as the standard protein, and the protein concentration in the sample was calculated by referencing the protein standard curve.

2.7.2. RNA quantitative analysis

RNA was quantified using spectrophotometry. The extinction coefficient ϵ (which represents the change in absorbance corresponding to the consumption of 1 g/L of RNA substrate in the reaction system) was calculated using Equation (Eq. 1). The experimental data and the fitted line are presented in the supporting materials (Fig. S1). The fitted extinction coefficient was determined to be $\epsilon = 19.63$. Based on this value, the amount of RNA consumed at any given time during the reaction with NP1 can be determined (Henderson, Benight, & Hanlon, 1992).

$$\text{Extinction coefficient } \epsilon = A/\omega \quad (1)$$

Notes: A: Absorbance of the enzymatic hydrolysis reaction system; ω : RNA concentration consumed in the enzymatic hydrolysis reaction system.

The reaction rates of NP1@CSMs-GA and free NP1 at various RNA concentrations were fitted according to the extinction coefficient. Finally, the kinetic parameters of the Michaelis-Menten equation for NP1@CSMs-GA and free NP1 were calculated using the Levenberg-Marquardt algorithm (Amini, Rostami, & Caristi, 2018), as shown in Equation (eq. 2)

$$\text{Michaelis - Menten Equation } V_{\max} = \frac{K_m \cdot [S]}{K_m + [S]} \quad (2)$$

2.7.3. Determination of protein loading capacity of CSMs prepared by various methods

Weigh 0.1 g of cross-linked activated CSMs prepared using the emulsification method, the neutralization method, and the combined emulsification-neutralization method, and place each sample into a 10 mL stoppered test tube. Add 5 mL of a 100 $\mu\text{g/mL}$ BSA solution to each tube, secure the tubes with stoppers, and incubate at 25 $^{\circ}\text{C}$ with 80 rpm for 2 h. After incubation, carefully decant the supernatant and wash the CSMs several times. Collect the washing solutions and combine them with the initial supernatant. Determine the BSA concentration in the combined solution using the Coomassie Brilliant Blue method (Buroker-Kilgore & Wang, 1993). The protein (BSA) loading ratio is then calculated based on the BSA concentration according to the following equation (Eq. 3):

$$\text{Protein loading ratio} = \left(1 - \frac{\text{BSA content in the solution after loading}}{\text{BSA content in the solution before loading}}\right) \times 100\% \quad (3)$$

2.7.4. Assay of Nuclease P1 activity

The activity of NP1 was assayed based on its ability to catalyze the hydrolysis of RNA into 5'-nucleotides, which have a characteristic absorption at 260 nm after the RNA precipitation process. One enzyme unit is defined as the amount of enzyme that produces a change in absorbance of 1.0 at 260 nm per minute under optimal catalytic conditions. (Ying, Shi, Zhang, Chen, & Yi, 2007; Zhuang et al., 2016).

The specific detection method for free NP1 and NP1@CSMs-GA activity is as follows: A specific volume of 3 % RNA solution (0.95 mL for

the free NP1 assay, or 3 mL for the NP1@CSMs-GA assay) was preheated in a thermostatic water bath at 80 $^{\circ}\text{C}$ for 5 min. Then, 0.05 mL of free NP1 solution (or 0.01 g of NP1@CSMs-GA) was added into the RNA solution, and the mixture was incubated for 5 min at 80 $^{\circ}\text{C}$. Next, 1 mL of nucleic acid precipitant (0.25 % ammonium molybdate-2.5 % perchloric acid) was added into the reaction mixture, which was then vigorously mixed. The mixture was immediately transferred to an ice bath and kept for 10 min. Then it was centrifuged, the supernatant was diluted to a specific multiple, and the absorbance at 260 nm was measured. The enzyme activity of free NP1 and NP1@CSMs-GA was calculated using the following equations (Eq. 4) and (Eq. 5). The yield of immobilized NP1 activity (Yield) was calculated based on equation (Eq. 6).

Enzyme activity of free NP1, EA (U/mL):

$$EA = \frac{(A - A_0) \times f \times 2 \times n}{0.05 \times 5} \quad (4)$$

Enzyme activity of NP1@CSMs-GA, EA_{im} (U/g):

$$EA_{im} = \frac{(A - A_0) \times 6 \times n}{0.01 \times 5} \quad (5)$$

Immobilization yield of NP1@CSMs-GA activity, Immobilization yield (%):

$$\text{Immobilization yield} = \frac{EA_{im}}{EA_0 - EA_1} \times 100 \quad (6)$$

Notes: A: Absorbance of the experimental group; A₀: The absorbance of the blank control group; f: Dilution ratio of enzyme solution; n: Dilution ratio of centrifuged supernatant of the reaction mixture; EA_{im}: Enzyme activity of NP1@CSMs-GA, U; EA₀: Total free NP1 activity before immobilization, U; EA₁: Left free NP1 activity after immobilization, U.

2.8. Statistical analysis

All experiments were performed in triplicate. The data represents the mean of triplicate values. The corresponding standard deviation was calculated. All statistical analyses were conducted using Excel (2021) and OriginPro (2021).

3. Results and discussion

3.1. Preparation of chitosan microspheres

Chitosan microspheres (CSMs) were prepared using three different methods: the emulsification method (Garncarek, 2019), the neutralization method (Ahmad et al., 2022), and the combined emulsification-neutralization method. Photographs of the corresponding microspheres are provided in the supplementary materials (Figs. S2). The particle size prepared by emulsion method is less than 1 μm , and the microspheres appear yellow and transparent. The microspheres pre-

pared by neutralization titration method are relatively large, with a milky white particle size of 3–4 μm . The microspheres prepared by combined emulsification-neutralization method have a particle size of about 0.5 μm . The protein loading capability of the CSMs prepared by the three methods was presented in Fig. 1A. The immobilization performance of the CSMs prepared by these three preparation methods to NP1 was preliminarily tested, and the relative enzyme activity of the NP1@CSMs and the immobilization activity yield is shown in Fig. 1B. The results indicated that the immobilization yield of NP1 with CSMs

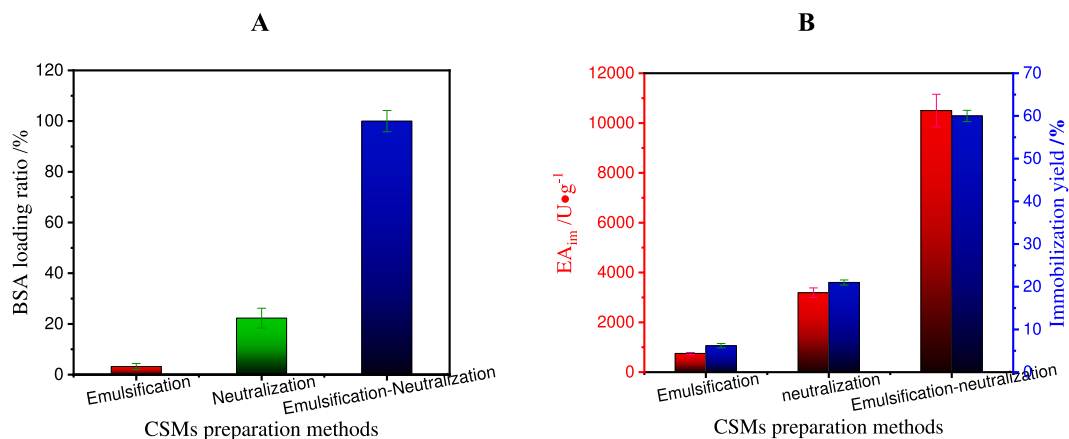


Fig. 1. Performance of CSMs (Chitosan Microspheres) prepared by various method. A: Protein loading capability; B: Immobilization performance to NP1 (Nuclease P1).

prepared by the combined emulsification-neutralization method exceeded 27 %, which was significantly higher than the yields from the single emulsification or neutralization methods. Based on the CSMs shape, size, and the protein loading capability, the combined emulsification-neutralization method was the most effective for CSMs preparation. Various crosslinking agents, including glutaraldehyde, epichlorohydrin, and polyethyleneimine (Virgen-Ortiz et al., 2017), were tested. Glutaraldehyde (GA) demonstrated the highest cross-linking efficiency based

on enzyme activity and immobilization yield, as shown in Fig. S3.

3.2. Immobilization of NP1@CSMs-GA

To achieve the optimal conditions for NP1 immobilization on CSMs-GA, we systematically investigated the impact of various immobilization reaction conditions, including temperature, pH, duration, NP1 quantity, and CSMs-GA amount, on the activity and immobilization yield of

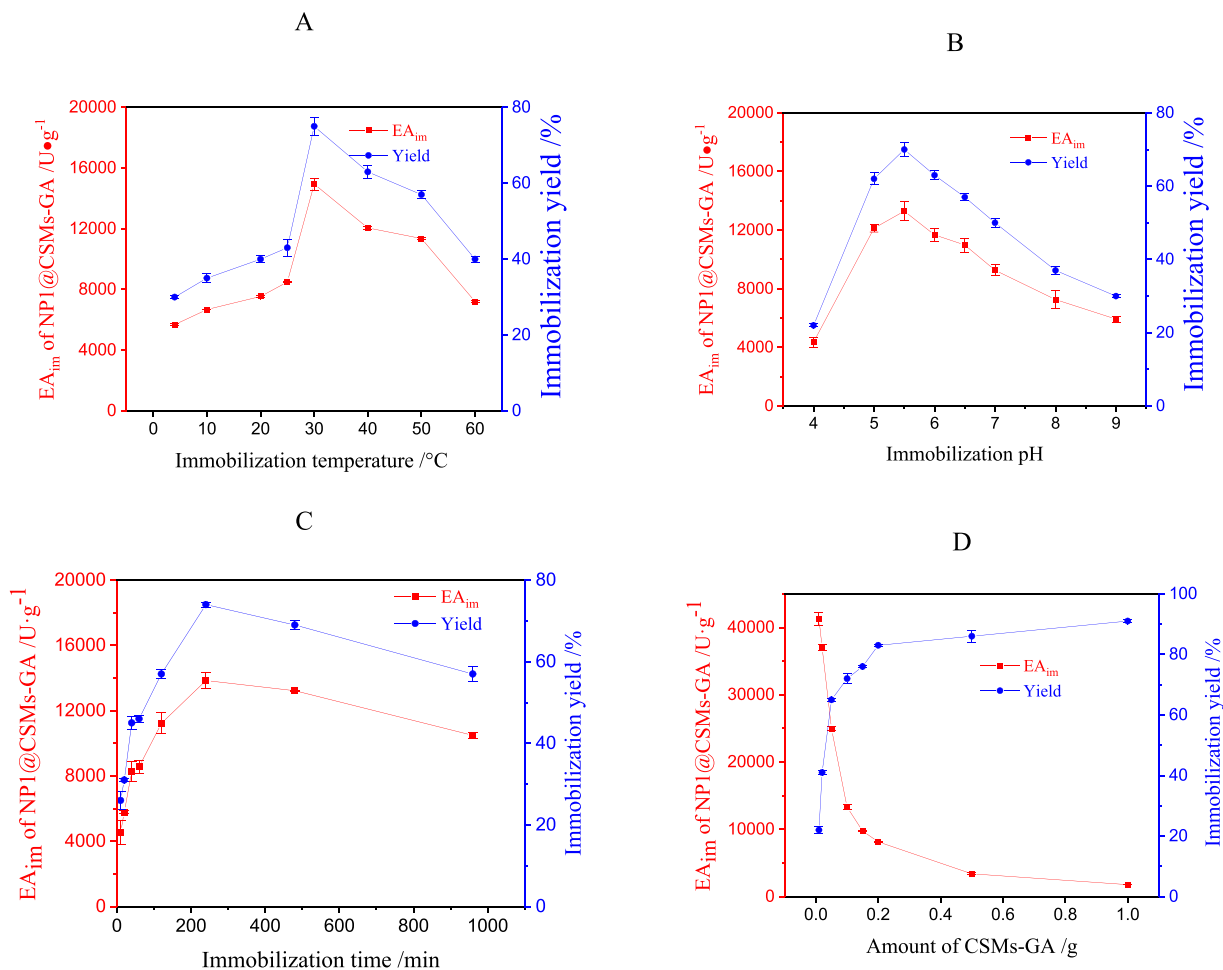


Fig. 2. Optimization of immobilization reaction conditions for NP1@CSMs-GA (NP1 immobilized on glutaraldehyde-cross-linked chitosan microspheres). A: Immobilization temperature; B: Immobilization pH; C: Immobilization time; D: Amount of CSMs-GA.

NP1@CSMs-GA. The results are illustrated in Fig. 2.

In Fig. 2A, both the relative activity of NP1@CSMs-GA and the immobilization yield peaked at 30 °C, suggesting that lower temperatures do not provide sufficient energy for the immobilization reaction process, while excessively high temperatures might lead to detrimental interactions between the functional groups of CSMs and the active sites of the enzyme (Colak & Gencer, 2012). Fig. 2B demonstrates that a pH of 5.5 was most conducive to the immobilization of NP1 onto CSMs-GA. It is similar to that of the immobilization of porcine pancreas trypsin onto chitosan-based nonwoven carriers (Kim & Lee, 2019). As depicted in Fig. 2C, the immobilization time of 4 h was sufficient to obtain the highest activity of NP1@CSMs-GA. Regarding the influence of CSMs quantity (Fig. 2D), the specific activity of NP1@CSMs-GA decreased with increasing amounts of CSMs, which aligns with previous expectations in porcine pancreas trypsin immobilization (Kim & Lee, 2019). Nonetheless, the immobilization yields initially rise before stabilizing, which indicate that the NP1 is effectively immobilized on CSMs-GA. Fig. 2E reveals a gradual increase in the activity of NP1@CSMs-GA with rising NP1 concentrations. The immobilization yields firstly decreased and then reached to a steady trend with rising NP1 concentration. During the optimization, it was found that using 0.5 g of CSMs-GA led to the highest activity recovery, at 75 %. Moreover, the maximum activity

of NP1@CSMs-GA, 53,859.4 U/g, was achieved when the NP1 concentration reached 131.56 µg/mL.

3.3. Characterization of NP1@CSMs-GA structure and composition

Scanning electron microscopy (SEM) was employed to analyze the microstructural characteristics of CSMs, CSMs-GA, and NP1@CSMs-GA, with the results summarized in Fig. 3. Specifically, Fig. 3A and B, C and D, and E and F illustrate the SEM images of CSMs, CSMs-GA, and NP1@CSMs-GA, respectively. Notably, the surface porosity and specific surface area of CSMs-GA are greater than those of CSMs. As depicted in Fig. 3B, visible cracks are present on the surface of CSMs. In contrast, following the cross-linking process, the surface of CSMs-GA appears more compact, as shown in Fig. 3D. Furthermore, Fig. 3F indicates that the surface of NP1@CSMs-GA remains well-structured, suggesting its robust mechanical properties (Saravanakumar et al., 2014; Srivastava & Anand, 2014).

To confirm the cross-linking of CSMs with GA and the subsequent binding of CSMs-GA with NP1, Fourier-transform infrared (FT-IR) spectroscopy was conducted. The FT-IR spectra of CSMs, CSMs-GA, and NP1@CSMs-GA are displayed in Fig. 4. After cross-linked with GA, the CSMs-GA exhibit distinct C—H stretching vibration peaks at 2928 cm⁻¹

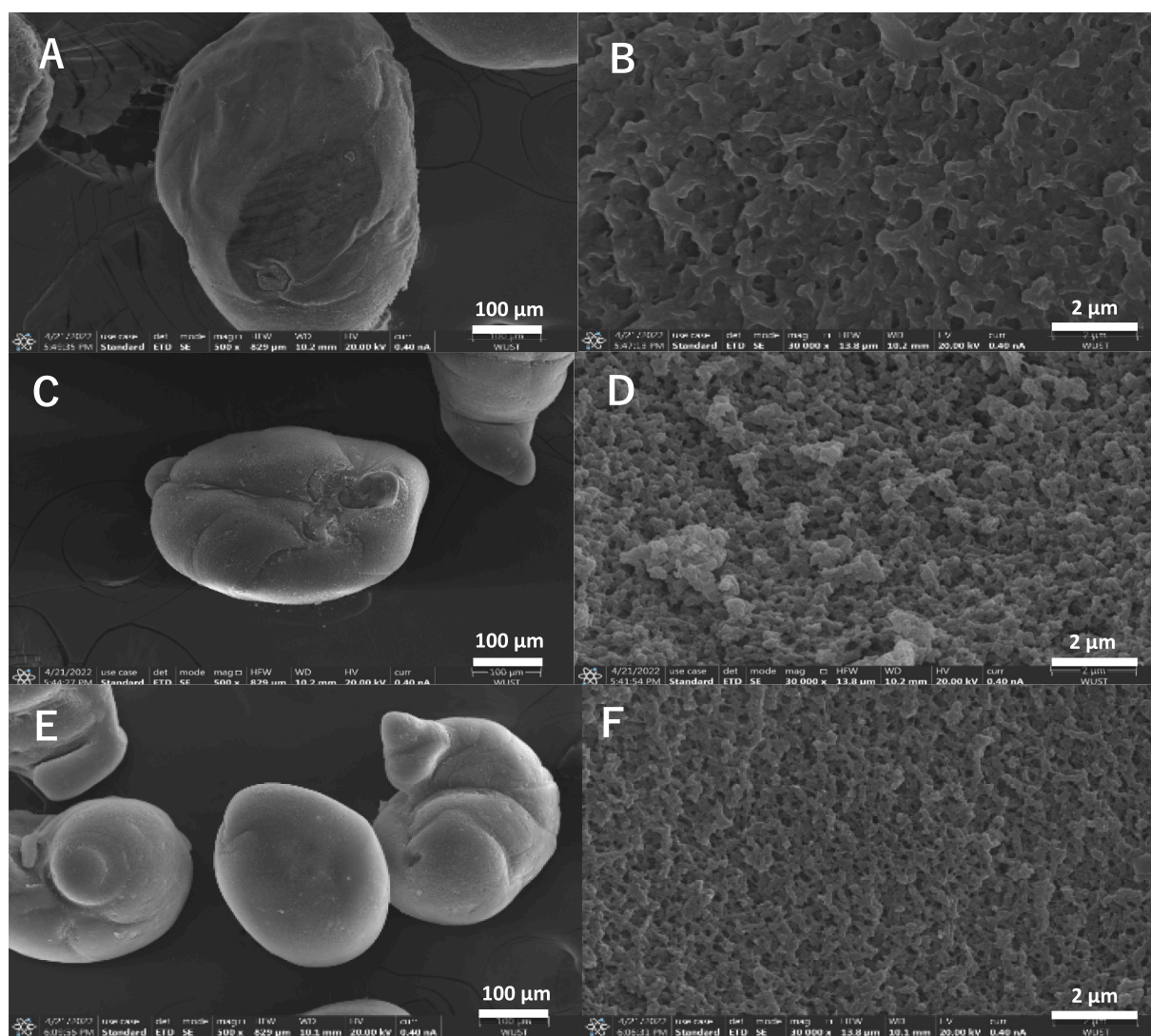


Fig. 3. SEM characterization of CSMs, CSMs-GA and NP1@CSMs-GA.

(A) SEM image of CSMs at 500 \times ; (B) SEM image of CSMs at 30000 \times ; (C) SEM image of CSMs-GA at 500 \times ; (D) SEM image of CSMs-GA at 30000 \times ; (E) SEM image of NP1@CSMs-GA at 500 \times ; (F) SEM image of NP1@CSMs-GA at 30000 \times .

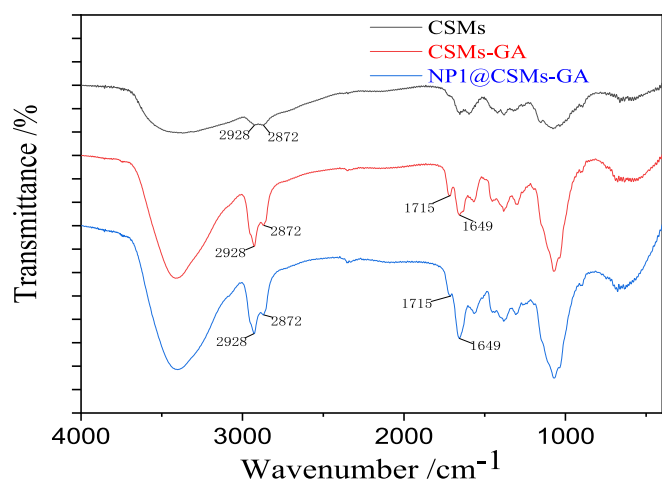


Fig. 4. FT-IR spectra of CSMs, CSMs-GA and NP1@CSMs-GA.

and 2872 cm^{-1} . Additionally, the presence of a C=O stretching vibration peak at 1715 cm^{-1} and a C=N stretching vibration peak at 1649 cm^{-1} confirms the successful cross-linking of chitosan with GA. These characteristic peaks demonstrate the free aldehyde groups and Schiff bases formed by the reaction of cross-linked chitosan microspheres (Singh, Singh, Suthar, & Dubey, 2011; Wang & Jiang, 2019). Upon comparing the C=O stretching vibration peak at 1715 cm^{-1} of NP1@CSMs-GA, which is notably weaker than that of CSMs-GA, and the C=N stretching vibration peak at 1649 cm^{-1} , which is relatively stronger, it is evident that the immobilization process leads to a reduction in free aldehyde groups and an increase in the number of Schiff bases. This supports the notion that the immobilization mechanism is based on Schiff base reactions, with GA serving as a linker between chitosan and NP1. Generally, the protein was linked to the carrier by Schiff base reaction between the free aldehyde group on the carrier and the amino group on the protein (Colak & Gencer, 2012; Wang & Jiang, 2019).

3.4. Enzymatic properties of NP1@CSMs-GA

The enzymatic properties of NP1@CSMs-GA, including the optimal temperature, pH, substrate concentration, stability, and kinetic parameters, were thoroughly assessed. For comparative purposes, the corresponding properties of free NP1 were also evaluated. The results, as depicted in Fig. 5, reveal that the enzymatic properties of NP1@CSMs-GA closely resemble those of free NP1. This suggests that the immobilization of NP1 on CSMs-GA does not significantly alter its intrinsic enzymatic properties, this finding consistent with the work of Colak and Gencer (Colak & Gencer, 2012) who immobilized paraoxonase on chitosan.

Notably, NP1@CSMs-GA demonstrated superior enzymatic performance over free NP1 regarding pH tolerance and substrate concentration. The abundance of amino and hydroxyl groups on the surface of CSMs-GA likely contributes to a buffering effect, enabling the enzyme to function across a broader pH range. Additionally, the immobilization process imparts greater structural rigidity and stability to NP1, allowing it to withstand more extreme pH conditions (Ying et al., 2007). Although free NP1 exhibits good storage stability at $4\text{ }^{\circ}\text{C}$, NP1@CSMs-GA displays even better long-term stability. After 50 days of storage at $4\text{ }^{\circ}\text{C}$, the residual activity of NP1@CSMs-GA was 63.23 %, highlighting a significant improvement in storage stability upon immobilization. A similar enhancement in stability has been observed in the case of immobilized acetylcholinesterase (Isik, 2020).

Kinetic parameters for both free NP1 and NP1@CSMs-GA were evaluated by measuring the initial reaction velocities at varying RNA (substrate) concentrations, with the data fitted to the Michaelis-Menten

equation. The outcomes are presented in Fig. 5E and F. The K_m values for free NP1 and NP1@CSMs-GA were 22.24 mg/mL and 77.27 mg/mL , respectively, while the v_{\max} values were $18.60\text{ mg/(mL}\cdot\text{min)}$ for free NP1 and $895.71\text{ mg/(g}\cdot\text{min)}$ for NP1@CSMs-GA. The increase in K_m for NP1@CSMs-GA post-immobilization can be attributed to two primary factors: a change in the conformation of NP1 molecules during the immobilization process, and an increase in substrate mass transfer resistance, which reduces the distribution coefficient between the matrix and the solution (Arsalan, Alam, Zofair, Ahmad, & Younus, 2020; Isik, 2020). Compare NP1 immobilized on other carriers, such as @nanoparticles K_m 8.06 mg/mL , @cellulose K_m 9.14 mg/mL (Ying et al., 2007;), @deae cellulose K_m 27.21 mg/mL (Shi, Yi, et al., 2010), @paper cellulose K_m 5.72 mg/mL and v_{\max} $0.16\text{ mg/(mL}\cdot\text{min)}$ (Shi, Tang, et al., 2010), and @macroporous absorbent resins K_m 18.125 mg/mL and v_{\max} $443.95\text{ U/(min}\cdot\text{mL)}$ (Li et al., 2012), the NP1@CSMs-GA shows high catalysis activity.

3.5. Application of NP1@CSMs-GA in nucleotide production

Production capacity is a critical factor for the practical application of an immobilized enzyme (Faria et al., 2021). For NP1, reports on its immobilization have been scarce, and even more so regarding the assessment of its production capability (Shi, Yi, et al., 2010; Ying et al., 2007; Zhuang et al., 2016). This study evaluated the production capacity of NP1@CSMs-GA through repeated cycles use in a BSTR and continuous operation in a PBR.

Fig. 6A illustrates the outcomes from the BSTR. Despite a gradual decline in activity with increased recycling use times, NP1@CSMs-GA still retained 75.1 % of its original activity after ten cycles. Enzyme activity loss during reuse is attributed not only to the elevated reaction temperature ($65\text{ }^{\circ}\text{C}$) but also to physical losses incurred during collection and washing after each cycle. Free nuclease P1 cannot be recycled or reused, so it can only undergo one hydrolysis RNA production reaction in a stirred tank reactor. On the other hand, the immobilized nuclease P1 (NP1@CSMs-GA) can keep with 75.1 % activity for 10 times. Based on the enzyme activity yield of 75 % prepared by immobilized nuclease P1, the utilization value of nuclease P1 increased by 539.6 % following just 10 cycles of reuse.

The catalytic performance of NP1@CSMs-GA in the continuous production of nucleotides within a PBR is illustrated in Fig. 6B. A constant stream of an RNA solution, with a concentration of 50 g/L , was fed into the reactor, where it was subjected to hydrolysis to generate nucleotides. The product concentration was monitored by taking periodic samples from the reactor's outlet, facilitating the calculation of the reaction rate. During the continuous operation, the RNA hydrolysis conversion rate sustained around 81 % of its original value even after 24 h, highlighting the exceptional operational stability and productivity of NP1@CSMs-GA. This robust performance lays a solid technical groundwork for transitioning the nucleotide industry's production processes from batch to continuous PBR operations. In comparison to batch processing, the PBR continuous operation offers several advantages, including enhanced production efficiency, consistent product quality, ease of automation, and better scalability. These benefits present a viable technological approach for the innovation of nucleotide production.

4. Conclusion

In this study, we successfully synthesized a novel type of chitosan microsphere (CSMs-GA) using an innovative emulsification-neutralization combination method and utilized it as a carrier for the immobilization of nuclease P1 (NP1). The immobilized enzyme, NP1@CSMs-GA, was achieved via a Schiff base reaction that effectively crosslinked the enzyme with the carrier. Through systematic optimization, we established the ideal conditions for both the preparation of CSMs-GA and the immobilization process. Under optimal conditions,

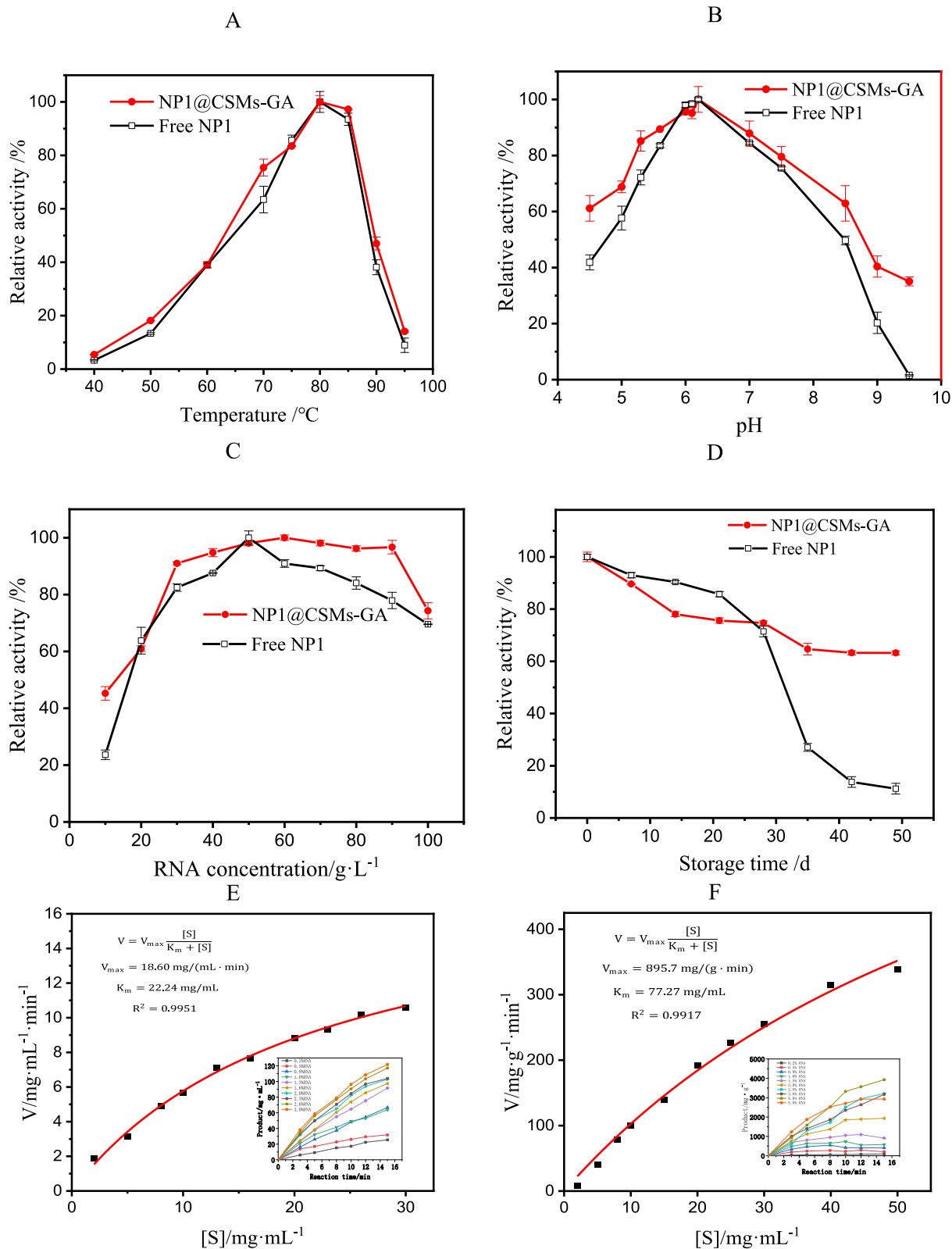


Fig. 5. Enzymatic properties of NP1@CSMs-GA and free NP1. A: Effect of temperatures on enzyme activity; B: Effect of pH on enzyme activity properties; C: Effect of RNA concentrations on enzyme activity; D: Storage stability; E: Kinetic parameters fitting of NP1; F: Kinetic parameters fitting of NP1@CSMs-GA.

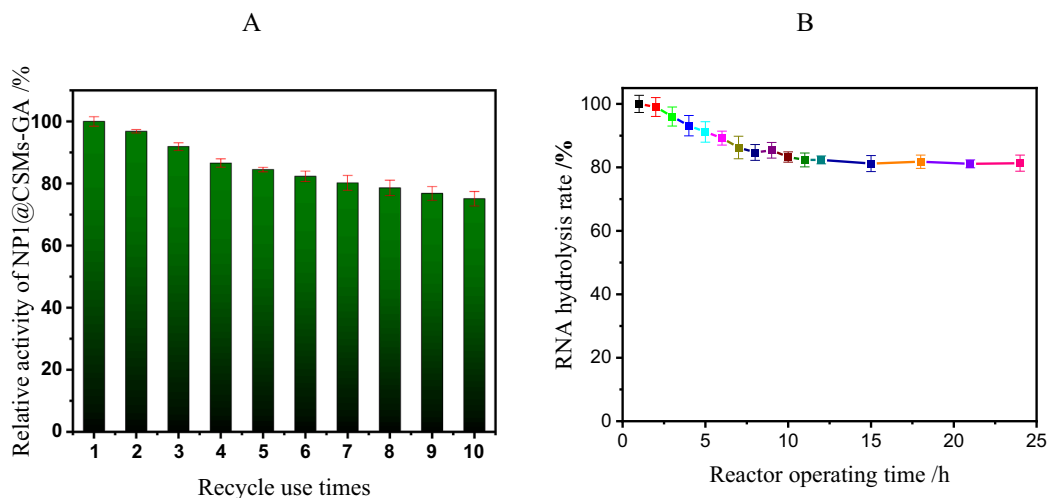


Fig. 6. Production performance of NP1@CSMs-GA.

A: repeated cycles use in a BSTR; B: continuous operation in a PBR.

NP1@CSMs-GA exhibited an activity of 41,000 U/g, with an enzyme activity recovery yield reaching up to 75 %.

Our findings demonstrate that compared to free NP1, NP1@CSMs-GA possesses superior enzymatic properties, including enhanced acid-base tolerance and storage stability. Importantly, the immobilized enzyme showed excellent operational performance in nucleotide production through RNA hydrolysis. In batch stirred tank reactors (BSTR), NP1@CSMs-GA maintained over 75.1 % of its initial activity after 10 cycles of reuse. Moreover, in a continuous packed-bed reactor (PBR), the enzyme retained approximately 81 % of its initial reaction rate after 24 h of continuous operation.

These results highlight NP1@CSMs-GA as a promising immobilized biocatalyst for nucleotide production, with potential applications not only in food processing but also in broader biotechnological fields. However, it is crucial to recognize that future research should focus on several key areas: Scalability, Cost Analysis, Optimizing Parameters for large-scale production, Expanding Applications. By addressing these areas, future studies can build upon our findings to enhance the practical utility and commercial viability of NP1@CSMs-GA, contributing significantly to the advancement of enzyme-based technologies.

Compliance with ethical standards

This article lacks research involving human or animal subjects.

CRediT authorship contribution statement

Xiao-Yan Yin: Writing – original draft, Methodology, Investigation.
Rui-Fan Yang: Writing – original draft, Data curation. **Zhong-Hua Yang:** Writing – review & editing, Funding acquisition, Conceptualization.

Declaration of competing interest

The authors declare that they have no known competing financial interests or personal relationships that could have appeared to influence the work reported in this paper.

Data availability

Data will be made available on request.

Acknowledgements

The authors acknowledge all the financial supports for this research by the Scientific Research Foundation for the Returned Overseas Chinese Scholars (State Education Ministry), the Key Project of Hubei Provincial Department of Science and Technology (2019AFB707).

Appendix A. Supplementary data

Supplementary data to this article can be found online at <https://doi.org/10.1016/j.fochx.2024.102130>.

References

- Ahmad, H., Garcia-Rogers, J., & Moreno, J. (2022). Preparation of magnetic chitosan beads as carriers for papain immobilization. *FASEB Journal*, 36(S1), L7859. <https://doi.org/10.1096/fasebj.2022.36.S1.L7859>
- Amini, K., Rostami, F., & Caristi, G. (2018). An efficient Levenberg-Marquardt method with a new LM parameter for systems of nonlinear equations. *Optimization*, 67(5), 637–650. <https://doi.org/10.1080/02331934.2018.1435655>
- Arsalan, A., Alam, M. F., Zofair, S. F. F., Ahmad, S., & Younus, H. (2020). Immobilization of beta-galactosidase on tannic acid stabilized silver nanoparticles: A safer way towards its industrial application. *Spectrochimica Acta Part a-Molecular and Biomolecular Spectroscopy*, 226, Article 117637. <https://doi.org/10.1016/j.saa.2019.117637>
- Atirog, V., Atiroglu, A., Atiroglu, A., Al-Hajri, A. S., & Özacar, M. (2024). Green immobilization: Enhancing enzyme stability and reusability on eco-friendly support. *Food Chemistry*, 448. <https://doi.org/10.1016/j.foodchem.2024.138978>
- Aydemir, T., & Guler, S. (2015). Characterization and immobilization of trametes versicolor laccase on magnetic chitosan-clay composite beads for phenol removal. *Artificial Cells, Nanomedicine, and Biotechnology*, 43(6), 425–432. <https://doi.org/10.3109/21691401.2015.1058809>
- Benaiges, M. D., López-Santin, J., & Solà, C. (1990). Production of 5'-ribonucleotides by enzymatic hydrolysis of RNA. *Enzyme and Microbial Technology*, 12(2), 86–89. [https://doi.org/10.1016/0141-0229\(90\)90078-5](https://doi.org/10.1016/0141-0229(90)90078-5)
- Buroker-Kilgore, M., & Wang, K. K. (1993). A Coomassie brilliant blue G-250-based colorimetric assay for measuring activity of calpain and other proteases. *Analytical Biochemistry*, 208(2), 387–392. <https://doi.org/10.1006/abio.1993.1066>
- Cavalcante, F. T. T., Cavalcante, A. L. G., de Sousa, I. G., Neto, F. S., & dos Santos, J. C. S. (2021). Current status and future perspectives of supports and protocols for enzyme immobilization. *Catalysts*, 11(10), 1222. <https://doi.org/10.3390/catal11101222>
- Chalella Mazzocato, M., & Jacquier, J.-C. (2024). Recent advances and perspectives on food-grade immobilisation systems for enzymes. *Foods*, 13(13), 2127. <https://doi.org/10.3390/foods13132127>
- Chen, S.-C., & Duan, K.-J. (2015). Production of galactooligosaccharides using beta-galactosidase immobilized on chitosan-coated magnetic nanoparticles with tris (hydroxymethyl)phosphine as an optional coupling agent. *International Journal of Molecular Sciences*, 16(6), 12499–12512. <https://doi.org/10.3390/ijms160612499>
- Colak, U., & Gencer, N. (2012). Immobilization of paraoxonase onto chitosan and its characterization. *Artificial Cells Blood Substitutes and Biotechnology*, 40(4), 290–295. <https://doi.org/10.3109/10731199.2011.652258>

- Collados, A., Conversa, V., Fombellida, M., Rozas, S., Kim, J. H., Arboleya, J.-C., ... Perezabad, L. (2020). Applying food enzymes in the kitchen. *International Journal of Gastronomy and Food Science*, 21, Article 100212. <https://doi.org/10.1016/j.ijgfs.2020.100212>
- Dutta, P. K., Ravikumar, M. N. V., & Dutta, J. (2002). Chitin and chitosan for versatile applications. *Journal of Macromolecular Science, Part C Polymer reviews*, 42(3), 307–354. <https://doi.org/10.1081/MC-120006451>
- Faria, L. L., Villalba Morales, S. A., Zanetti Prado, J. P., Dias, G. d. S., de Almeida, A. F., Abreu Xavier, M. D. C., ... Perna, R. F. (2021). Biochemical characterization of extracellular fructosyltransferase from *Aspergillus oryzae* IPT-301 immobilized on silica gel for the production of fructooligosaccharides. *Biotechnology Letters*, 43(1), 43–59. <https://doi.org/10.1007/s10529-020-03016-7>
- Garncarek, J. B.-B. Z. (2019). Immobilization of naringinase from *Penicillium decumbens* on chitosan microspheres for debittering grapefruit juice. *Molecules*, 24(23), 4234. <https://doi.org/10.3390/molecules24234234>
- Henderson, J. T., Benight, A. S., & Hanlon, S. (1992). A semi-micromethod for the determination of the extinction coefficients of duplex and single-stranded-DNA. *Analytical Biochemistry*, 201(1), 17–29. [https://doi.org/10.1016/0003-2697\(92\)90169-8](https://doi.org/10.1016/0003-2697(92)90169-8)
- Hoang Hiep, N., & Kim, M. (2017). An overview of techniques in enzyme immobilization. *Applied Science and Convergence Technology*, 26(6), 157–163. <https://doi.org/10.5757/asct.2017.26.6.157>
- Isik, M. (2020). High stability of immobilized acetylcholinesterase on chitosan beads. *Chemistryselect*, 5(15), 4623–4627. <https://doi.org/10.1002/slct.202000559>
- Kim, J. S., & Lee, S. (2019). Immobilization of trypsin from porcine pancreas onto chitosan nonwoven by covalent bonding. *Polymers*, 11(9), 1462. <https://doi.org/10.3390/polym11091462>
- Krajewska, B. (2004). Application of chitin- and chitosan-based materials for enzyme immobilizations: A review. *Enzyme and Microbial Technology*, 35(2/3), 126–139. <https://doi.org/10.1016/j.enzmictec.2003.12.013>
- Li, B., Chen, Y., Chen, X., Liu, D., Niu, H., Xiong, J., ... Ying, H. (2012). A novel immobilization method for nuclease P1 on macroporous absorbent resin with glutaraldehyde cross-linking and determination of its properties. *Process Biochemistry*, 47(4), 665–670. <https://doi.org/10.1016/j.procbio.2012.01.008>
- Liu, H., Xu, Y., Liang, K., & Liu, R. (2020). Immune cells combined with nlrp3 inflammasome inhibitor exert better antitumor effect on pancreatic ductal adenocarcinoma. *Frontiers in Oncology*, 10, 1378. <https://doi.org/10.3389/fonc.2020.01378>
- Nunes, Y. L., de Menezes, F. L., de Sousa, I. G., Cavalcante, A. L. G., Cavalcante, F. T. T., da Silva Moreira, K., ... dos Santos, J. C. S. (2021). Chemical and physical chitosan modification for designing enzymatic industrial biocatalysts: How to choose the best strategy? *International Journal of Biological Macromolecules*, 181, 1124–1170. <https://doi.org/10.1016/j.ijbiomac.2021.04.004>
- Raveendran, S., Parameswaran, B., Ummalyma, S. B., Abraham, A., Mathew, A. K., Madhavan, A., ... Pandey, A. (2018). Applications of microbial enzymes in food industry. *Food Technology and Biotechnology*, 56(1), 16–30. <https://doi.org/10.17113/ftb.56.01.18.5491>
- Ribeiro, E. S., de Farias, B. S., Sant'Anna Cadaval Junior, T. R., de Almeida Pinto, L. A., & Diaz, P. S. (2021). Chitosan-based nanofibers for enzyme immobilization. *International Journal of Biological Macromolecules*, 183, 1959–1970. <https://doi.org/10.1016/j.ijbiomac.2021.05.214>
- Rodrigues, R. C., Berenguer-Murcia, A., Carballares, D., Morellon-Sterling, R., & Fernandez-Lafuente, R. (2021). Stabilization of enzymes via immobilization: Multipoint covalent attachment and other stabilization strategies. *Biotechnology Advances*, 52, Article 107821. <https://doi.org/10.1016/j.biotechadv.2021.107821>
- da S. Moreira, K., Barros de Oliveira, A. L., Saraiva de Moura Júnior, L., Germano de Sousa, I., Luthierre Gama Cavalcante, A., Simão Neto, F., ... dos Santos, J. C. S. (2022). Taguchi design-assisted co-immobilization of lipase A and B from *Candida antarctica* onto chitosan: Characterization, kinetic resolution application, and docking studies. *Chemical Engineering Research and Design*, 177, 223–244. <https://doi.org/10.1016/j.chemd.2021.10.033>
- Saravananakumar, T., Palvannan, T., Kim, D.-H., & Park, S.-M. (2014). Optimized immobilization of peracetic acid producing recombinant acetyl xylan esterase on chitosan coated-Fe₃O₄ magnetic nanoparticles. *Process Biochemistry*, 49(11), 1920–1928. <https://doi.org/10.1016/j.procbio.2014.08.008>
- Shi, L.-E., Tang, Z.-X., Yi, Y., Chen, J.-S., Wang, H., Xiong, W.-Y., & Ying, G.-Q. (2010). Study of immobilization of nuclease p1 on paper cellulose. *Biotechnology and Biotechnological Equipment*, 24(3), 1997–2003. <https://doi.org/10.2478/V10133-010-0043-1>
- Shi, L.-E., Yi, Y., Tang, Z.-X., Xiong, W.-Y., Mei, J.-F., & Ying, G.-Q. (2010). Nuclease P1 immobilized on deae cellulose. *Brazilian Journal of Chemical Engineering*, 27(1), 31–39. <https://doi.org/10.1590/s0104-66322010000100003>
- Shi, L.-E., Ying, G.-Q., Tang, Z.-X., Chen, J.-S., Xiong, W.-Y., & Wang, H. (2009). Continuous enzymatic production of 5'-nucleotides using free nuclease P1 in ultrafiltration membrane reactor. *Journal of Membrane Science*, 345(1–2), 217–222. <https://doi.org/10.1016/j.memsci.2009.09.001>
- Singh, A. N., Singh, S., Suthar, N., & Dubey, V. K. (2011). Glutaraldehyde-activated chitosan matrix for immobilization of a novel cysteine protease, procerain B. *Journal of Agricultural and Food Chemistry*, 59(11), 6256–6262. <https://doi.org/10.1021/jf200472x>
- Srivastava, P. K., & Anand, A. (2014). Immobilization of acid phosphatase from *vigna aconitifolia* seeds on chitosan beads and its characterization. *International Journal of Biological Macromolecules*, 64, 150–154. <https://doi.org/10.1016/j.ijbiomac.2013.11.023>
- Virgen-Ortiz, J. J., dos Santos, J. C. S., Berenguer-Murcia, A., Barbosa, O., Rodrigues, R. C., & Fernandez-Lafuente, R. (2017). Polyethylenimine: A very useful ionic polymer in the design of immobilized enzyme biocatalysts. *Journal of Materials Chemistry B*, 5(36), 7461–7490. <https://doi.org/10.1039/c7tb01639e>
- Wang, D., & Jiang, W. (2019). Preparation of chitosan-based nanoparticles for enzyme immobilization. *International Journal of Biological Macromolecules*, 126, 1125–1132. <https://doi.org/10.1016/j.ijbiomac.2018.12.243>
- Wu, H.-L., Gong, Y., Ji, P., Xie, Y.-F., Jiang, Y.-Z., & Liu, G.-Y. (2022). Targeting nucleotide metabolism: A promising approach to enhance cancer immunotherapy. *Journal of Hematology & Oncology*, 15(1), 45. <https://doi.org/10.1186/s13045-022-01263-x>
- Ying, Q.-Q., Shi, L.-E., Zhang, X.-Y., Chen, W., & Yi, Y. (2007). Characterization of immobilized nuclease P1. *Applied Biochemistry and Biotechnology*, 136(1), 119–126. <https://doi.org/10.1007/bf02685942>
- Yushkova, E. D., Nazarova, E. A., Matyuhina, A. V., Noskova, A. O., Shavronskaya, D. O., Vinogradov, V. V., ... Krivoschapkina, E. F. (2019). Application of immobilized enzymes in food industry. *Journal of Agricultural and Food Chemistry*, 67(42), 11553–11567. <https://doi.org/10.1021/acs.jafc.9b04385>
- Zhang, J., Liu, D., Liu, J., Han, Y., Xu, H., Leng, X., ... Liu, L. (2020). Hybrid spherical nucleotide nanoparticles can enhance the synergistic anti-tumor effect of CTLA-4 and PD-1 blockades. *Biomaterials Science*, 8(17), 4757–4766. <https://doi.org/10.1039/d0bm00908c>
- Zhang, W., Shao, Z. Q., Wang, Z. X., Ye, Y. F., Li, S. F., & Wang, Y. J. (2024). Advances in aldo-keto reductases immobilization for biocatalytic synthesis of chiral alcohols. *International Journal of Biological Macromolecules*, 274, Article 133264. <https://doi.org/10.1016/j.ijbiomac.2024.133264>
- Zhou, X., Zhang, W., Zhao, L., Gao, S., Liu, T., & Yu, D. (2023). Immobilization of lipase in chitosan-mesoporous silica material and pore size adjustment. *International Journal of Biological Macromolecules*, 235, Article 123789. <https://doi.org/10.1016/j.ijbiomac.2023.123789>
- Zhuang, W., He, L., Zhu, J., Zheng, J., Liu, X., Dong, Y., ... Ying, H. (2016). Efficient nanobiocatalytic systems of nuclease P-1 immobilized on PEG-NH₂ modified graphene oxide: Effects of interface property heterogeneity. *Colloids and Surfaces. B, Biointerfaces*, 145, 785–794. <https://doi.org/10.1016/j.colsurfb.2016.05.074>